



A simplified micromechanical model for predicting effective mechanical behaviors of continuous bidirectional-fiber-reinforced composites

Wu-Gui Jiang, Zhi-Kai Wu, Long Zheng & Qing H. Qin

To cite this article: Wu-Gui Jiang, Zhi-Kai Wu, Long Zheng & Qing H. Qin (2017) A simplified micromechanical model for predicting effective mechanical behaviors of continuous bidirectional-fiber-reinforced composites, *Mechanics of Advanced Materials and Structures*, 24:15, 1292-1299, DOI: [10.1080/15376494.2016.1227505](https://doi.org/10.1080/15376494.2016.1227505)

To link to this article: <http://dx.doi.org/10.1080/15376494.2016.1227505>



Accepted author version posted online: 31 Aug 2016.
Published online: 31 Aug 2016.



Submit your article to this journal [↗](#)



Article views: 67



View related articles [↗](#)



View Crossmark data [↗](#)

ORIGINAL ARTICLE



A simplified micromechanical model for predicting effective mechanical behaviors of continuous bidirectional-fiber-reinforced composites

Wu-Gui Jiang^{a,b}, Zhi-Kai Wu^a, Long Zheng^a, and Qing H. Qin^b

^aSchool of Aeronautical Manufacturing Engineering, Nanchang Hangkong University, Nanchang, China; ^bResearch School of Engineering, Australian National University, Canberra, Australia

ABSTRACT

A simplified micromechanical model is proposed to estimate the macroscopic mechanical properties of continuous bidirectional-fiber-reinforced composites (CBFRCs) by ignoring Poisson's effect. The model is validated by results from a homogenized finite element approach. Based on the proposed analytical model, the influences of the ratios of fiber/matrix modulus and the fiber volume ratio on the effective modulus and the tensile strength are specifically investigated. The suggested theoretical method provides a convenient tool for estimating the effective mechanical behaviors of CBFRCs, which can be expressed as a function of fiber volume fraction and material parameters.

ARTICLE HISTORY

Received 18 March 2016
Accepted 24 June 2016

KEYWORDS

Bi-directional-fiber-reinforced composite; effective elastic modulus; homogenized finite element method; micromechanics; tensile strength

1. Introduction

As a type of important composites, fiber-reinforced composite (FRC) materials have been widely received as a broad range of applications from household devices to aeronautics industries because of their outstanding physical, mechanical, and thermal properties, in particular their high stiffness and strength-to-weight ratio [1–6]. Usually, when fibers are embedded into a matrix to form a composite, the physical and mechanical properties of the FRC depend on the properties of the composite's constituents and the corresponding geometry and concentration. Unlike unidirectional fiber-reinforced composites (UFRCs), bidirectional-fiber-reinforced composites (BFRCs) can have specified in-plane mechanical properties along two distinct in-plane directions.

During the past decades much work has been done to study effects of unidirectional fibers on effective properties of composites. Based on the finite element (FE) and homogenization method, a representative volume element (RVE) has been used to estimate the effective macroscopic mechanical properties of UFRCs [7, 8]. Alternatively, a set of analytical formulae obtained from some straightforward methods has been utilized to estimate effective mechanical properties of UFRCs. Existing theoretical methods for predicting macroscopically effective properties of composites include the dilute model [9], self-consistent method [10], a combination of the Mori-Tanaka method and the iso-strain and iso-stress assumptions [11], a generalized self-consistent method [12], and Christensen's approach [13]. An elementary mechanics of materials model was presented by Gibson [14] for predicting four independent effective moduli of orthotropic continuous unidirectional fiber-reinforced lamina.

It should be mentioned that study of BFRCs has been less popular than that of UFRCs. A bidirectional carbon-fiber-reinforced zirconia matrix composite was fabricated recently by slurry infiltration and hot pressing techniques and its mechanical properties and microstructure were measured [15]. Dong and Davies [16] investigated the flexural strength of bidirectional fiber-reinforced epoxy composites using the FE method. To the authors' knowledge, however, micromechanics-based analytical models for predicting effective modulus and tensile strength of BFRCs have not yet been reported.

The purpose of this study is to develop a micromechanics-based analytical model for estimating the effective elastic modulus and tensile strengths of continuous BFRCs (CBFRCs) using a homogenization FE method. Specifically, the influences of Poisson's ratio, the modulus ratio of fiber over matrix, and the fiber content on the effective mechanical behaviors are investigated.

2. Simplified micromechanics model

2.1. Geometrical description

Figure 1a shows a schematic diagram of a cross-ply composite reinforced by fibers along two perpendicular directions. On the basis of the assumption of a homogenization method, this CBFRC is simplified as a structure with periodically and uniformly distributed unit cells, as shown in Figure 1b. An enlarged unit cell (also called RVE) is shown in Figure 1c. Since Wu et al. [17] already discussed the interfacial effect on the effective properties of the CBFRCs via the finite element method, perfect bonding at the interface is assumed here for the sake of

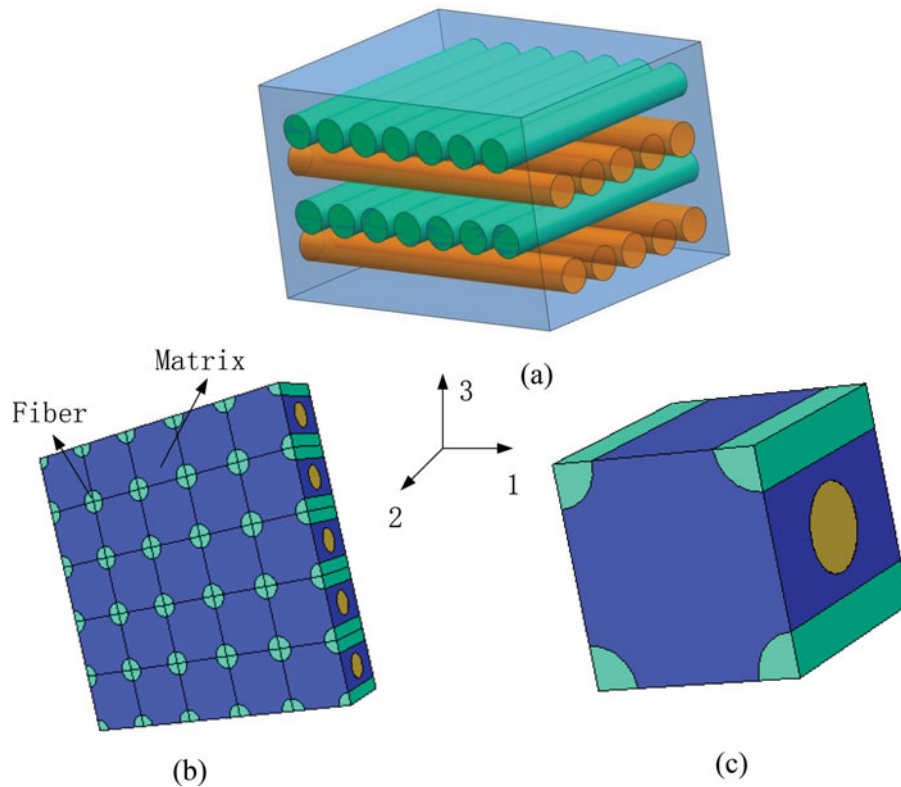


Figure 1. (a) Schematic diagram of cross-ply composite reinforced by fibers along two directions, (b) sketch of fiber-reinforced composites, and (c) homogenized 3D unit cell.

simplicity. This assumption has been widely used in estimating the effective properties via the analytical method [14, 18–20] and the finite element method [21–23].

2.2. Effective modulus

If we assume that the fiber spacing, s , and the fiber diameter, d , do not change along the fiber length, then the area fraction is equal to the volume fraction, as shown in Figure 2a. Following the approach of Hopkins and Chamis [24], the RVE in Figure 2b can be changed into that shown in Figure 2c.

The equivalent square fiber shown in Figure 2c has the following dimensions:

$$l_f = \sqrt{\frac{\pi}{4}} d \quad (1)$$

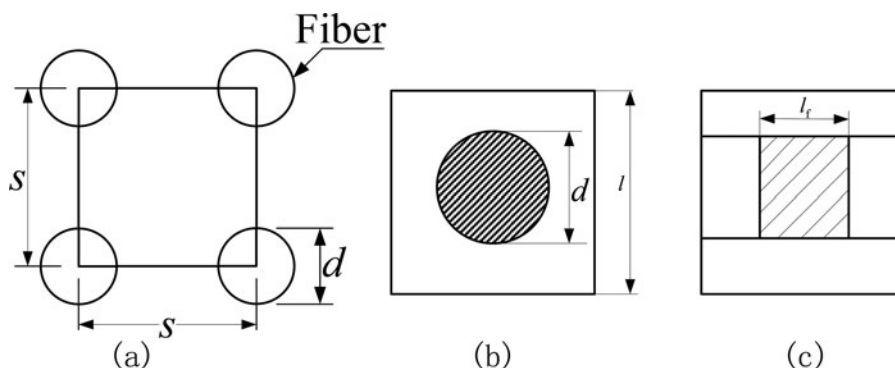


Figure 2. (a) Idealized fiber-packing composite, (b) representative area element, and (c) division of representative area element into subregions based on a square fiber having a fiber volume fraction equivalent to that of a round fiber.

where d and l_f are the diameter of the original circular fiber and the side length of the refined square fiber, respectively.

The constituent volume fraction in the RVE is assumed to be the same as those in the actual composite. For CBFRCs, therefore, the original RVE shown in Figure 1c can be redrawn as that shown in Figure 3, and then its region can be divided into subregions A, B, and C. In subregion A the fiber is parallel to 2-axis and in subregion C the fiber is parallel to 1-axis. In subregion B there is no fiber in the matrix. Following the assumptions of fiber and matrix, the RVE of CBFRCs is macroscopically homogeneous, linearly elastic, and orthotropic, respectively. We define directions 1 and 2 as in-plane directions and direction 3 as an out-of-plane direction, as shown in Figure 3.

Figure 4 shows the finite element contour plots of stress components in the case of fibers subject to a tension along 1-axis, where the fiber volume fraction is 25%, $E_f = 300$ GPa, $E_m =$

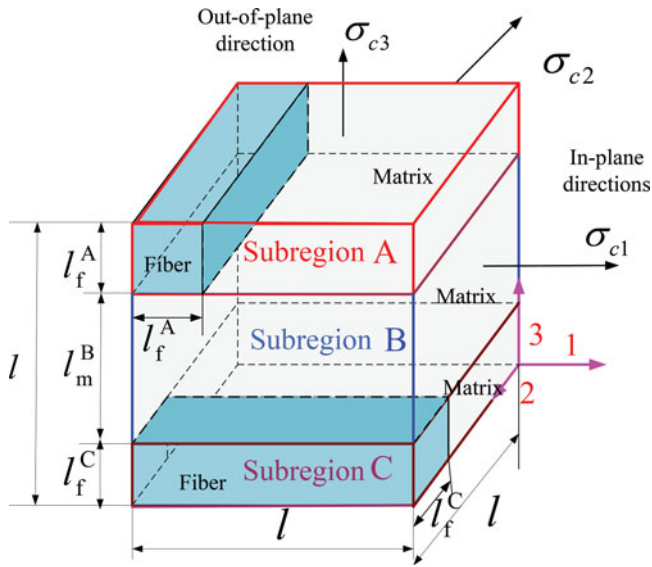


Figure 3. Subregion sketch of the unit cell in the proposed analytical model under simple stress states.

100 GPa, and the tensile strain is 0.34%. It can be seen that the shear stresses are far less than the normal stress along the tensile direction in the two fibers when the composites are subject to a tension. Thus, we ignore the shear stress effect in our simplified micromechanics model.

When the RVE in **Figure 3** is subjected to an in-plane normal stress, σ_{c1} or σ_{c2} , as shown in **Figure 3**, its response is governed by the effective in-plane modulus, E_{c1} and E_{c2} .

For subregion A, if the structure is subjected to a transverse normal stress, σ_{c1} , as shown in **Figure 3**, the effective modulus is governed by the effective transverse modulus, E_1^A . Geometric compatibility requires that the total transverse composite displacement, δ_{c1}^A , must equal the sum of the corresponding transverse displacements in the fiber, δ_{f1}^A , and the matrix, δ_{m1}^A :

$$\delta_{c1}^A = \delta_{f1}^A + \delta_{m1}^A, \quad (2)$$

$$\delta_{c1}^A = \varepsilon_{c1}l, \delta_{f1}^A = \varepsilon_{f1}l_f^A, \delta_{m1}^A = \varepsilon_{m1}l_{m1}^A, \quad (3)$$

where l_f^A , l_{m1}^A , and l are the side length of the fiber, the matrix in the subregion A, and the RVE along direction l . ε represents normal strain. The subscripts c, f, and m refer to composite, fiber, and matrix, respectively; the subscript l refers to the direction l ; and the superscript A refers to subregion A. Therefore, Eq. (2) now becomes:

$$\varepsilon_{c1}l = \varepsilon_{f1}l_f^A + \varepsilon_{m1}l_{m1}^A. \quad (4)$$

Since the dimensions of the subregion A do not change along the 2 direction, the length fractions must equal to the volume fraction and Eq. (4) can be rearranged to get the rule of mixtures for transverse strains:

$$\varepsilon_{c1} = \varepsilon_{f1}L_f^A + \varepsilon_{m1}L_m^A, \quad (5)$$

where L_f^A , L_m^A represent fiber volume fraction and matrix volume fraction in subregion A, respectively.

The one-dimensional (1D) Hooke's laws for this case are:

$$\sigma_{c1}^A = E_1^A \varepsilon_{c1}, \sigma_{f1}^A = E_f \varepsilon_{f1}, \sigma_{m1}^A = E_m \varepsilon_{m1}, \quad (6)$$

where E_f and E_m represent the elastic moduli of fiber and matrix phases, respectively. Herein, the Poisson strains have been neglected. Combining Eqs. (5) and (6), we get:

$$\frac{\sigma_{c1}^A}{E_1^A} = \frac{\sigma_{f1}^A}{E_f} L_f^A + \frac{\sigma_{m1}^A}{E_m} L_m^A. \quad (7)$$

If we assume that the stresses in the composite, matrix, and the fiber are all equal, Eq. (7) reduces to the "inverse rule of mixtures" for the transverse modulus:

$$\frac{1}{E_1^A} = \frac{1}{E_f} L_f^A + \frac{1}{E_m} L_m^A, \quad (8)$$

where L_f^A and L_m^A satisfy:

$$L_f^A + L_m^A = 1. \quad (9)$$

The effective transverse modulus for this subregion is found to be:

$$E_1^A = \frac{E_m}{1 - L_f^A(1 - E_m/E_f)}. \quad (10)$$

When the structure is subjected to σ_{c1} in subregion C, static equilibrium requires that the total resultant force on the element equals the sum of the forces acting on the fiber and matrix. Thus, we obtain the relation between the stress in composite, fiber, and matrix as:

$$\sigma_{c1}^C A_1^C = \sigma_{f1}^C A_f^C + \sigma_{m1}^C A_m^C, \quad (11)$$

where A refers to the loading area, and the superscript C refers to subregion C. As area fractions are equal to the corresponding volume fraction L , Eq. (6) can be rearranged for longitudinal stress as:

$$\sigma_1^C = E_1^C \varepsilon_{c1}; \quad \sigma_{f1}^C = E_f \varepsilon_{f1}; \quad \sigma_{m1}^C = E_m \varepsilon_{m1}. \quad (12)$$

All materials follow a one-dimensional (1D) Hooke's law (i.e., Poisson's strain is neglected).

Then Eq. (11) becomes:

$$E_1^C \varepsilon_{c1} = E_f \varepsilon_{f1} L_f^C + E_m \varepsilon_{m1} L_m^C, \quad (13)$$

where E_1^C , L_f^C , and L_m^C represent the effective longitudinal elastic modulus, fiber volume fraction, and matrix volume fraction in subregion C, respectively.

Assuming that the strains in the composite, fiber, and matrix along direction l are equal, we obtain the mixture rule for the longitudinal modulus from Eq. (13):

$$E_1^C = E_f L_f^C + E_m L_m^C, \quad (14)$$

where L_f^C and L_m^C satisfy:

$$L_f^C + L_m^C = 1. \quad (15)$$

According to the mixture rule, the macro equivalent modulus in direction l is expressed as:

$$E_{c1} = E_1^A \frac{V_A}{V_{A+B+C}} + E_m \frac{V_B}{V_{A+B+C}} + E_1^C \frac{V_C}{V_{A+B+C}}, \quad (16)$$

where V_A , V_B , V_C , and V_{A+B+C} are the volumes of subregions A, B, C, and the whole RVE, respectively.

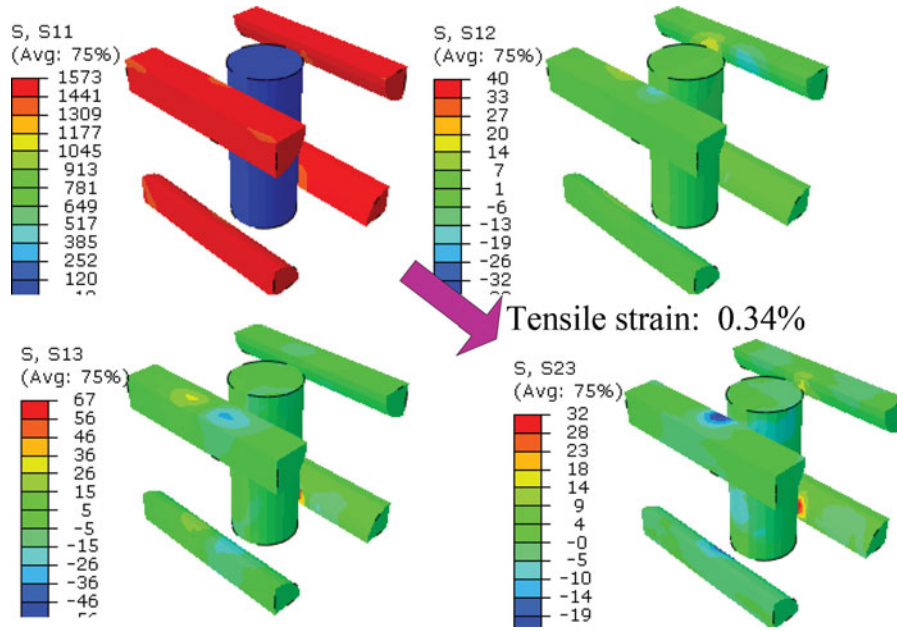


Figure 4. Finite element contour plots of stress components of fibers subject to a tension along I -axis, where the fiber volume fraction is 25%, $E_f = 300$ GPa, $E_m = 100$ GPa, and the tensile strain is 0.34%.

Similarly, we can obtain the macro effective elastic modulus E_{c2} in direction 2 in the same way.

If the RVE is subjected to an out-of-plane normal stress, σ_{c3} , as mentioned previously, we can obtain the effective out-of-plane elastic modulus along direction 3, i.e.:

$$E_{c3} = E_m \left[(1 - \sqrt{L_f}) + \frac{\sqrt{L_f}}{1 - \sqrt{L_f} (1 - E_m/E_f)} \right], \quad (17)$$

where the total fiber volume L_f in the whole RVE is expressed as:

$$L_f = \left(\frac{l_f}{l} \right)^2 = \frac{(l_f^A)^2 + (l_f^C)^2}{l^2}. \quad (18)$$

2.3. Effective tensile strengths

As shown in Figure 5, the linear stress-strain relationship for the composites is simplified by the use of the concept of “effective modulus.” Similarly, the “effective strength” of the composites may be defined as ultimate values of volume-averaged stresses that cause failure of the composites under the same simple states of stress.

The model first proposed by Hull and Clyne [1] is described briefly here for the convenience of the subsequent discussion. In the analysis, we assume that (1) strength is equal for all fibers, (2) fiber and matrix behavior are all linear elastic until their stress reaches the tensile strength, and (3) equal strains exist in composite, fiber, and matrix. Figure 5 shows the case where the fiber failure strain is greater than the matrix failure strain. Composite failure will occur at the strain level corresponding to the matrix tensile strain, $e_m^{(+)}$. Thus, when the matrix stress reaches the matrix tensile strength, $s_m^{(+)}$, the fiber stress reaches the value $s_{fm}^{(+)} = E_f e_m^{(+)}$, and the composite stress reaches the composite strength, $s^{(+)}$.

When a certain load is applied in direction 1, subregion A is subjected to a transverse normal stress. A strain concentration factor F developed by Kies [25] is introduced for calculating the corresponding transverse failure strain:

$$e_T^{(+)} = e_m^{(+)} / F, \quad (20)$$

where the strain concentration F is valid when $E_f/E_m \geq 1$.

For subregion A, the strain concentration factor F_A can be expressed as:

$$F_A = \frac{1}{\frac{l_f^A}{l} (E_m/E_f - 1) + 1} = \frac{1}{L_f^A (E_m/E_f - 1) + 1}. \quad (21)$$

Note that $F \geq 1$ when $E_f/E_m \geq 1$, so $e_T^{(+)} \leq e_m^{(+)}$. Here, we only consider the case that the fiber failure strain is greater than

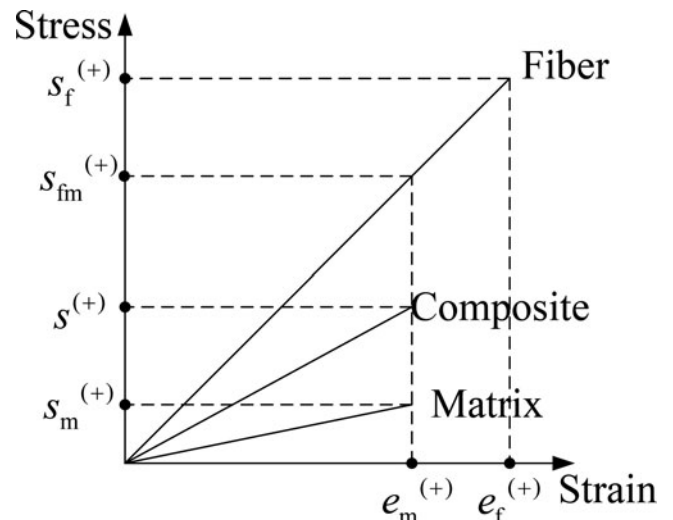


Figure 5. Representative stress-strain curves for typical fiber, matrix, and composite materials, where fiber failure strain is greater than matrix failure strain.

the matrix failure strain. The failure of the RVE structure shown in Figure 3 can be divided into three stages as follows:

- (i) When the loading strain equals to $e_T^{(+)}$, subregion A fails first; at that time both subregions B and C do not reach their maximum carrying capacities. The tensile strength of the composites, $s_{cl}^{I(+)}$, can be expressed as:

$$s_{cl}^{I(+)} = s_{T1}^{A(+)} \frac{V_A}{V_{A+B+C}} + E_m e_T^{(+)} \frac{V_B}{V_{A+B+C}} + (E_f L_f^C + E_m L_m^C) e_T^{(+)} \frac{V_C}{V_{A+B+C}}, \quad (22)$$

where the corresponding transverse strength $s_{T1}^{A(+)}$ of subregion A under σ_{cl} is:

$$s_{T1}^{A(+)} = \frac{E_1^A s_m^{(+)}}{E_m F_A}. \quad (23)$$

- (ii) When the loading strain equals to $e_m^{(+)}$, subregion B and the matrix in subregion C fail; at that time subregion A cannot carry any loads. We assume that the Young's modulus E of subregion A is degraded to 1% from its initial value. The degradation percentage values are selected based on values similar to those used by Dodds et al. [26] and by Blacketter et al. [27] via correlating them to experimental data. The tensile strength of the composites $s_{cl}^{II(+)}$ can be expressed as:

$$s_{cl}^{II(+)} = 0.01 s_{T1}^{A(+)} \frac{V_A}{V_{A+B+C}} + s_m^{(+)} \frac{V_B}{V_{A+B+C}} + (E_f L_f^C + E_m L_m^C) e_m^{(+)} \frac{V_C}{V_{A+B+C}}. \quad (24)$$

- (iii) When the loading strain reaches $e_f^{(+)}$, the fibers in subregion C fail finally; at that time the Young's moduli of subregions A and B and the matrix in subregion C are degraded to 1% from their initial values. The tensile strength of the composites $s_{cl}^{III(+)}$ can be expressed as:

$$s_{cl}^{III(+)} = 0.01 s_{T1}^{A(+)} \frac{V_A}{V_{A+B+C}} + 0.01 s_m^{(+)} \frac{V_B}{V_{A+B+C}} + (E_f L_f^C + 0.01 E_m L_m^C) e_f^{(+)} \frac{V_C}{V_{A+B+C}}, \quad (25)$$

where $e_f^{(+)} = \frac{s_f^{(+)}}{E_f}$.

The transverse tensile strength of the CBFRCs is determined by:

$$s_{cl}^{(+)} = \text{Max} \left(s_{cl}^{I(+)}, s_{cl}^{II(+)}, s_{cl}^{III(+)} \right). \quad (26)$$

Similarly, the macro in-plane tensile strength in direction 2 can be calculated in a similar way to $s_{cl}^{(+)}$.

The out-of-plane tensile strength in direction 3 is:

$$s_{c3}^{(+)} = \frac{E_{c3} s_m^{(+)}}{E_m F}, \quad (27)$$

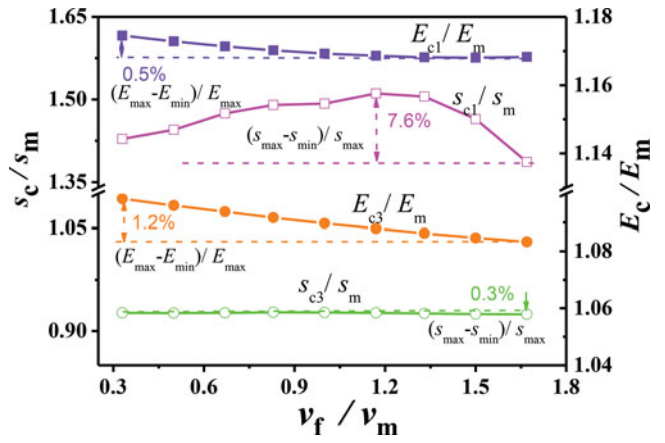


Figure 6. Influence of Poisson's ratio on the effective elastic constants and tensile strengths.

where the strain concentration factor F for the whole unit cell in direction 3 is:

$$F = \frac{1}{\frac{l_f}{l} (E_m/E_f - 1) + 1} = \frac{1}{\sqrt{L_f} (E_m/E_f - 1) + 1}. \quad (28)$$

3. Results and discussion

3.1. Effect of Poisson's ratio

As mentioned before, we ignored the influence of Poisson's ratio on the macro elastic modulus and the tensile strength. Here, FE simulations are performed to analyze the influence of Poisson's ratio on elastic modulus and tensile strength.

The curves of elastic modulus and tensile strength with respect to the fiber Poisson's ratio are shown in Figure 6, where the Young's moduli of matrix and fiber are assumed to be 100 and 300 GPa, respectively, and the Poisson's ratio of the matrix is assumed to be 0.3. In our simulation, the dimensions of the RVE are set to be $1 \times 1 \times 1$. Here, the diameter of the fiber is set to be 0.2 and 0.4, respectively (i.e., the fiber volume fraction is set to be 6 and 25%, respectively) in estimation of the elastic moduli and the tensile strengths, respectively. The Poisson's ratio of the fiber varies in the range of 0.1–0.5. The tensile and compressive strengths of the fiber are assumed to be the same, 2000 MPa, while the tensile and compressive strengths of the matrix are 200 and 2000 MPa, respectively. We define the influence rate of Poisson's ratio as the absolute ratio value of the difference between the maximum FE value and the minimum FE value to the maximum FE value for the cases of different Poisson's ratios. From Figure 6 we find that the influence rate of the in-plane tensile strength ratio (IPTSR) reaches 7.6%, those of the remaining parameters including the out-of-plane tensile strength ratio (OPTSR), the in-plane modulus ratio (IPMR), and the out-of-plane modulus ratio (OPMR) are less than 1.2%, indicating that the Poisson's ratio has little impact on the macro elastic modulus and tensile strengths, so it is ignored in our analysis.

3.2. Comparison of the analytical and FE approaches

Using the proposed approach, we determined the effective elastic moduli and tensile strengths of CBFRCs, where $L_f = 25\%$, $E_f = 300\text{GPa}$, $E_m = 100\text{GPa}$, and $v_m = v_f = 0.3$.

To examine the accuracy of the results from the theoretical method above, a FE RVE model with homogeneous boundary conditions is set up to validate our proposed analytical model. It is noted that boundary conditions can significantly affect the effective properties of the RVEs during the homogenization simulations. Two types of boundary conditions are generally used in the literature. If an RVE with 3D periodic boundary conditions (PBCs) is used, the simulation results represent a macro structure consisting of periodically repeated cells. While choosing 3D homogeneous boundary conditions (HBCs), the simulation results would consider the RVE as the macro structure itself with its micro-constituents. HBCs are used in our simulations. The detailed description on the HBCs is referred to our previous work [28]. The macroscopically effective mechanical properties can be determined through the estimation of one unit cell at fine scale. The analytical estimation on the elastic moduli and strengths is based on the simplified square cross-sectional fibers, but original circular cross-sectional fibers are still built in the RVE used in our FE simulations, as shown in Figure 1c. The side length of the equivalent square fiber is expressed as a function of the diameter of the original circular fiber, as given in Eq. (1). For simplicity, the fiber volumes are assumed to be the same in directions 1 and 2 during the simulations. We assume that the fibers along the two directions do not overlap each other, so the fiber volume fraction, L_f , does not exceed 40%.

The fiber and matrix should be linear elastic when the stress level is below their tensile strength. If the stress level exceeds the maximum strength for matrix and/or fiber, the Young's modulus E is assumed to be degraded to 1% from its initial value at a particular integration point and the shear modulus G is assumed to be reduced to 20% of its initial value under the assumption that some shear stiffness remains due to the friction still present on the failure plane. As mentioned above, the degradation percentage values are selected based on values similar to those used by Dodds et al. [26] and by Blacketter et al. [27] via correlating them to experimental data. These assumptions can be easily realized through use of the user subroutine USDFLD in ABAQUS.

Table 1 shows that all the effective elastic moduli and tensile strengths predicted from the present theoretical model have a good agreement with our FEM results. Therefore, all of the discussion below will be based on the theoretical method presented in Section 2.

3.3. Effect of fiber content

The overall material elastic modulus and tensile strength are usually improved via increasing the volume fraction of fibers in the matrix for UFRCs, but for BFRCs it is still unclear how those values are affected by the fiber content. In this section we consider the influence of fiber volume fraction on the overall elastic

Table 1. Comparison of the present analytical model and FEM results.

	IPMR (E_{c1}/E_m)	OPMR (E_{c3}/E_m)	IPTSR (s_{c1}/s_m)	OPTSR (s_{c3}/s_m)
FEM result	1.384	1.289	1.310	0.858
Analytical result	1.163	1.251	1.270	0.833
Relative error	1.662%	2.984%	3.053%	2.914%

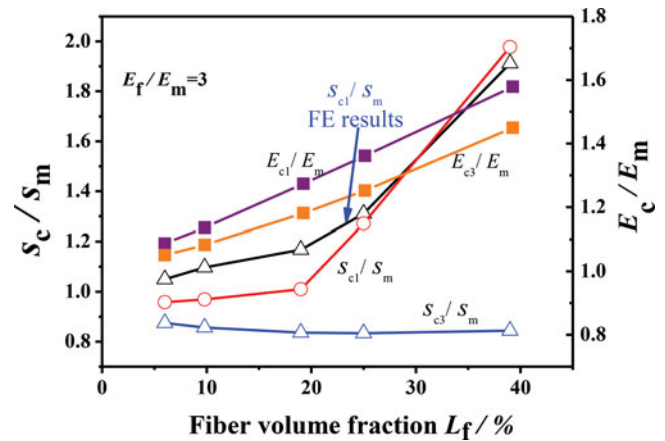


Figure 7. Influence of fiber content on effective elastic constant and tensile strength, where the fiber volume fraction $L_f = 25\%$.

modulus and tensile strength. Because square fibers are simplified in our proposed model, we assume that the fibers do not overlap each other for simplicity. It should be mentioned, however, that the proposed micromechanical model can be used to determine the effective properties of the composites in the case that fibers along two directions overlap each other. The fiber volumes are assumed to be the same in directions 1 and 2, so the fiber volume fraction L_f does not exceed 40%. The fiber volume fraction L_f^A varies from 0 to 44.3% in subregion A, and L_f^C varies from 0 to 44.3% in subregion C, i.e., the fiber volume fraction L_f in the RVE varies from 0 to 39.3%.

The influence of the fiber content on elastic constant and tensile strength is shown in Figure 7, where $E_f/E_m = 3$. For comparison, the curve of the IPTSRs obtained from the finite element simulations is also listed in Figure 7. Figure 7 shows that both the IPMR and the OPMR of the composites increase sharply as the fiber volume fraction increases, and it also illustrates that the OPTSR of the CBFRCs is insensitive to the fiber volume fraction, whereas the IPTSR increases sharply as the fiber volume fraction increases, satisfying the mixture rule. From Figure 7, we note that there exists a change in slope of the curves of the IPTSRs obtained from both the analytical model and the finite element simulations at 19.2% fiber volume fraction. This is because the composite in-plane tensile strength is determined by Eq. (22) when the fiber volume fraction is less than 19.2%, while it would be given by Eq. (25) when the fiber volume fraction exceeds 19.2%.

3.4. Effect of ratio of fiber/matrix modulus

Figure 8a plots the change trends of analytical macroscopic elastic constants of the CBFRCs with respect to modulus ratio E_f/E_m ranging from 1 to 5, where $L_f = 6\%$, $L_f = 25\%$, respectively. With the increase of the ratio E_f/E_m , the OPMR and IPMR increase gradually, but the curve of the fiber content $L_f = 25\%$ is sharper than the fiber content $L_f = 6\%$. With the increase of the fiber content and modulus ratio E_f/E_m , the values of IPMR and OPMR differ as they grow.

The curves of the in-plane and out-of-plane tensile strength with respect to the modulus ratio E_f/E_m ranging from 1 to 5 are plotted in Figure 8b. It can be seen that the IPTSR is almost independent of E_f/E_m , whereas the OPTSR decreases gradually

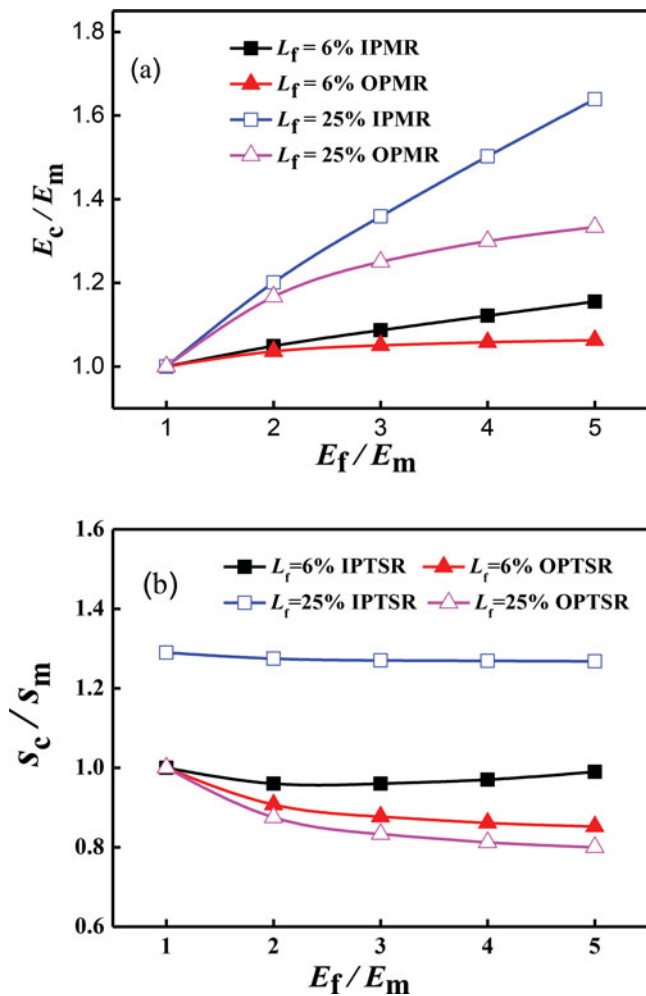


Figure 8. Influence of the modulus ratio of fiber to matrix on: (a) effective elastic constants and (b) tensile strengths.

with the increase of E_f/E_m . The curve of IPTSR is always above the OPTSR.

4. Conclusions

A simplified RVE micromechanical model is proposed to estimate the effective macroscopic mechanical properties of CBFRCs by ignoring the Poisson's effect, and is then validated by a homogenized FE model. Using the proposed model, the influences of Poisson's ratio, the ratio of fiber/matrix modulus E_f/E_m , and the fiber volume fraction L_f on the effective modulus and tensile strength are investigated in turn.

The results obtained from the proposed model show good agreement with the numerical results from the FE method. Our FE results show that the Poisson's ratio of fiber and matrix has little impact on the macro elastic modulus in all directions. We found that the modulus ratio of fiber and matrix can significantly influence the in-plane macro elastic modulus and out-of-plane tensile strength of the composite but have little impact on the macro out-of-plane elastic modulus and in-plane tensile strength. With the increase of fiber content, the macro in-plane and out-of-plane elastic moduli and the in-plane tensile strength increase dramatically, whereas the out-of-plane tensile strength decreases slightly.

The suggested theoretical method provides a convenient tool for estimating the effective elastic modulus and tensile strength of CBFRCs, as a function of fiber volume fraction and material parameters and, therefore, is valuable for the optimal design of CBFRCs with enhanced performance.

Funding

This work was supported by the National Natural Science Foundation of China (Grant No. 11372126).

References

- [1] D. Hull and T. Clyne, *An Introduction to Composite Materials*, Cambridge University Press, Cambridge, 1996.
- [2] J.K. Kim and Y.W. Mai, High strength, high fracture toughness fibre composites with interface control—A review, *Compos. Sci. Technol.*, vol. 41, no. 4, pp. 333–378, 1991.
- [3] S. Chand, Review carbon fibers for composites, *J. Mater. Sci.*, vol. 35, no. 6, pp. 1303–1313, 2000.
- [4] Q.H. Qin, Introduction to the composite and its toughening mechanisms. In: *Toughening Mechanisms in Composite Materials*, Q.H. Qin and J.Q. Ye, Eds., pp. 1–32, Elsevier, Cambridge, 2015.
- [5] Z. Hu and R. Karki, Prediction of mechanical properties of three-dimensional fabric composites reinforced by transversely isotropic carbon fibers, *J. Compos. Mater.*, vol. 49, no. 12, pp. 1513–1524, 2015.
- [6] R.W. Davidge, *Fiber-reinforced ceramics*, *Composites*, vol. 18, no. 2, pp. 92–98, 1987.
- [7] D.F. Adams and D.A. Crane, Finite element micromechanical analysis of a unidirectional composite including longitudinal shear loading, *Comput. Struct.*, vol. 18, no. 6, pp. 1153–1165, 1984.
- [8] Q.H. Qin and Q.S. Yang, *Macro-Micro Theory on Multifield Coupling Behavior of Heterogeneous Materials*, Springer, Berlin, 2008.
- [9] Q.H. Qin and M.V. Swain, A micro-mechanics model of dentin mechanical properties, *Biomaterials*, vol. 25, no. 20, pp. 5081–5090, 2004.
- [10] W.G. Jiang, J.L. Yao, J.M. Peng, and H.P. Zhao, Finite element and molecular dynamics models for predicting effective mechanical behaviors of carbon nanotube bundles, *Acta Mech.*, vol. 225, no. 12, pp. 3549–3558, 2014.
- [11] X.Q. Feng, Y.W. Mai, and Q.H. Qin, A micromechanical model for interpenetrating multiphase composites, *Comput. Mater. Sci.*, vol. 28, no. 3, pp. 486–493, 2003.
- [12] S. Yu and Q.H. Qin, Damage analysis of thermopiezoelectric properties: Part II. Effective crack model, *Theor. Appl. Mech.*, vol. 25, no. 3, pp. 279–288, 1996.
- [13] R.M. Christensen and K.H. Lo, Solutions for effective shear properties in three phase sphere and cylinder models, *J. Mech. Phys Solids*, vol. 27, no. 4, pp. 315–330, 1979.
- [14] R.F. Gibson, *Principles of Composite Material Mechanics*, CRC Press, Boca Raton, 2011.
- [15] J. Ai, G. Zhou, H. Zhang, P. Liu, Z. Wang, and S. Wang, Mechanical properties and microstructure of two-dimensional carbon fiber reinforced zirconia composites prepared by hot-pressing, *Ceram. Int.*, vol. 40, no. 1, pp. 835–840, 2014.
- [16] C. Dong and I.J. Davies, Flexural strength of bidirectional hybrid epoxy composites reinforced by E glass and T700S carbon fibres, *Composites Part B*, vol. 72, pp. 65–71, 2015.
- [17] Z.K. Wu, W.G. Jiang, and L. Zheng, The interfacial effect on mechanical behaviors of bidirectional-fiber-reinforced composites, *Acta Mater. Compos. Sin.*, vol. 34, no. 1, pp. 217–223, 2017.
- [18] S.Y. Fu, X. Hu, and C. Yoon, A new model for the transverse modulus of unidirectional fiber composites, *J. Mater. Sci.*, vol. 33, no. 20, pp. 4953–4960, 1998.
- [19] S.Y. Fu and B. Lauke, The elastic modulus of misaligned short-fiber-reinforced polymers, *Compos. Sci. Technol.*, vol. 58, no. 3–4, pp. 389–400, 1998.

- [20] Z.M. Huang, Micromechanical prediction of ultimate strength of transversely isotropic fibrous composites, *Int. J. Solids. Struct.*, vol. 38, no. 22–23, pp. 4147–4172, 2001.
- [21] A. Taliercio and R. Coruzzi, Mechanical behaviour of brittle matrix composites: A homogenization approach, *Int. J. Solids. Struct.*, vol. 36, no. 24, pp. 3591–3615, 1999.
- [22] J.M.M. Dekok and H.E.H. Meijer, Deformation, yield and fracture of unidirectional composites in transverse loading: 1. Influence of fibre volume fraction and test-temperature, *Composites Part A*, vol. 30, no. 7, pp. 905–916, 1999.
- [23] I. Ivanov and A. Tabiei, Three-dimensional computational micro-mechanical model for woven fabric composite, *Compos. Struct.*, vol. 54, no. 4, pp. 489–496, 2001.
- [24] D.A. Hopkins and C.C. Chamis, A unique set of micromechanics equations for high-temperature metal matrix composites. In: *Testing Technology of Metal Matrix Composites*, ASTM STP 964, Philadelphia: American Society for Testing and Materials, p. 159–76, 1988.
- [25] J. Kies, Maximum strains in the resin of fiberglass composites, DTIC Document, 1962.
- [26] R.H. Dodds, L.A. Lopez, and D.A. Pecknold, Numerical and software requirements of general nonlinear finite element analysis, Report No. UIIU-ENG-78-2020, University of Illinois at Urbana-Champaign, 1978.
- [27] D. Blacketter, D. Walrath, and A. Hansen, Modeling damage in a plain weave fabric-reinforced composite material, *J. Compos. Technol. Res.*, vol. 15, no. 2, pp. 136–142, 1993.
- [28] W.G. Jiang, R.Z. Zhong, Q.H. Qin, et al., Homogenized finite element analysis on effective elastoplastic mechanical behaviors of composite with imperfect interfaces, *Int. J. Mol. Sci.*, vol. 15, no. 12, pp. 23389–23407, 2014.